Quick transport of primary produced organic carbon to the ocean interior

M. C. Honda,[1] H. Kawakami,[1] K. Sasaoka,[2] S. Watanabe,[1] and T. Dickey[3]

Received 31 March 2006; revised 15 June 2006; accepted 27 June 2006; published 17 August 2006.

[1] Time-series observations of optical fields in the euphotic layer and particle fluxes at 150 m were made in the western North Pacific for half year of 2005. The ratio of surface photosynthetically available radiation (surface PAR) to in situ quantum irradiance at *ca.* 40 m (in situ QI), as an index of turbidity, began to increase in the middle of April, peaking between the end of June and the middle of July. Seasonal variability in the ratio of spectral irradiance at a wavelength of 555 nm to that at 443 nm ($Ed_{(555)}/Ed_{(443)}$) at 40 m, as an index of chlorophyll abundance, synchronized well with the surface PAR/in situ QI ratio. Organic carbon flux also increased between the end of June and the middle of July and correlated well with optical variability. This result suggests that primary produced carbon in the euphotic layer was quickly transported to the ocean interior. Using the $Ed_{(555)}/Ed_{(443)}$ and an empirical equation from shipboard observations, primary productivity was estimated to be *ca.* 300 mgC m^{-2} day^{-1} on average. Assuming that trapping efficiency was only 20% and organic carbon flux decreased drastically between 100 m and 150m, the export ratio at 100 m was estimated to be *ca.* 30 ± 10%, which is significantly higher than that in other oceans. **Citation:** Honda, M. C., H. Kawakami, K. Sasaoka, S. Watanabe, and T. Dickey (2006), Quick transport of primary produced organic carbon to the ocean interior, *Geophys. Res. Lett.*, *33*, L16603, doi:10.1029/2006GL026466.

1. Introduction

[2] To better understand the oceans' ability to uptake atmospheric CO_2, the downward transport of carbon via the "biological pump" mechanism needs to be quantified [e.g., *Volk and Hoffert*, 1985]. Time-series data collected using sediment trap has been effectively used for this purpose [e.g., *Honjo et al.*, 1999]. However, sediment traps have usually been deployed in the deep sea (>1000 m). Therefore, concern has been expressed about how well deep sediment trap data represents the biological activity in the upper layer. Interestingly, progress in satellite oceanography has enabled us to learn about spatial and temporal variation of biological activity [e.g., *Banse and English*, 1999]. Unfortunately, ocean color data provides only near surface information and the existence of clouds often hampers acquisition of satellite color data, especially for the coastal and high latitude region. Thus, we chose to simultaneously observe and quantify biological activity in the euphotic layer using in situ optical sensors and particle fluxes just below the winter mixed layer with a sediment trap. These concurrent observations have enabled the establishment of linkages and correlations between upper and deeper ocean biological and biogeochemical processes.

2. Experimental Procedure and Methods

[3] A bottom tethered mooring system was deployed at station K2 (47°N, 160°E, water depth 5280 m) in the Western Subarctic Gyre (WSG). The WSG has large seasonal variability in physical, chemical and biological parameters [*Harrison et al.*, 2004]. Seasonal surface water temperature and mixed layer range from *ca.* 1°C and *ca.* 100 m in winter to >10°C and *ca.* 30 m in summer, respectively. In late spring, primary productivity increases with temperature, light intensity and water stratification. Seasonal drawdown of nutrients from late winter to early autumn is larger than that in other oceans. The euphotic layer is relatively constant (*ca.* 50 m) and diatom numerically predominates the phytoplankton assemblage year round. A time-series sediment trap (McLane Mark7G) with 21 collecting cups was installed at 150 m that is *ca.* 50 m below the late winter mixed layer at station K2 (M. C. Honda, unpublished data, 2005). Sampling of settling particles began on 20 March 2005 and ceased on 11 September 2005. The particle collecting interval was 14 days for the first 4 cups and 7 days for the remaining 17 collecting cups. Collected samples were preserved with seawater based buffered 5% formalin. After pretreatment of samples, the concentrations of organic carbon were measured with an elemental analyzer and concentrations of Si, Ca and Al were measured with ICP-AES, and converted to organic materials, opal, $CaCO_3$ and lithogenic materials, respectively following *Honda et al.* [2002]. In order to estimate trapping efficiency, ^{230}Th and ^{232}Th was measured using the α counting method [*Anderson and Fleer*, 1982]. The Bio-optical Long-term Optical Ocean Measuring System (BLOOMS [*Dickey et al.*, 2003]) which consists of a Satlantic Inc. spectral radiometer [OCR-504-ICWS] with data acquisition/storage systems was installed for measurement of downwelling spectral irradiance (Ed) at 4 wavelengths (412, 443, 490, and 555 nm). The depth of BLOOMS measured with a depth sensor (RIGO DP1158) was stable during the experimental period (37.5 ± 2.0 m on average). The optical system was kept free of biofouling by copper shutters [*Manov et al.*, 2004]. The values of Ed at 4 wavelengths were measured every hour during the local daytime period (19:00–7:00 UTC)

[1]Mutsu Institute for Oceanography, Japan Agency for Marine-Earth Science and Technology, Yokosuka, Japan.
[2]Frontier Research Center for Global Change, Japan Agency for Marine-Earth Science and Technology, Yokohama, Japan.
[3]Ocean Physics Laboratory, University of California, Santa Barbara, Goleta, California, USA.

0094-8276/06/2006GL026466$05.00

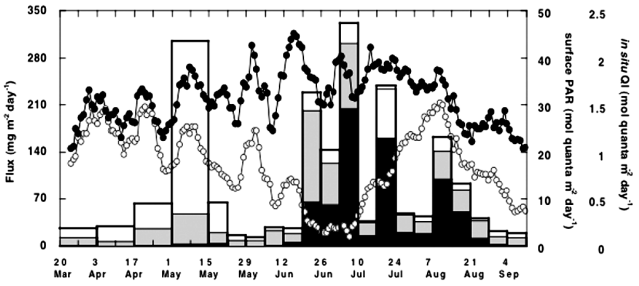

Figure 1. Sinking particles fluxes (bar graphs), and 7 days running mean of surface PAR (closed circles) based on optical data from SeaWiFS and in situ quantum irradiance spectra (QI: open circles). White, stripe, gray and black bars are fluxes of carbonate, lithogenic materials, organic materials, and biogenic opal, respectively.

from 20 March 2005 to 20 September 2005. The daily in situ quantum irradiance spectra (in situ QI) (mol quanta cm^{-2} sec^{-1}) between 412 and 555 nm were calculated from the Ed at 4 wavelengths following *Sorensen and Siegel* [2001].

3. Results

3.1. Fluxes of Settling Particles at 150 m

[4] The first increase of total mass flux (TMF) was observed in early May (Figure 1). The concentration of $CaCO_3$ for particles collected by mid-May was >50%. The main contributor to $CaCO_3$ flux was foraminiferal shell. After late June, TMF increased again with maximum values in early July. Compared to chemical compositions of the early settling particles, biogenic opal (mainly diatom testa) was predominant. Mean TMF was 96 mg m^{-2} day^{-1}. This value seemed too small compared to average TMF observed in the deep sea for the WSG (*ca.* 100 mg m^{-2} day^{-1} at 1000 m [*Honda et al.*, 2002]). Average flux of ^{230}Th was 0.0021 dpm m^{-2} day^{-1} or 0.76 dpm m^{-2} yr^{-1}. Assuming steady state and no effect of laterally transported ^{230}Th, ^{230}Th flux after subtracting authigenic ^{230}Th flux based on ^{232}Th was only 20 ± 7% of the expected ^{230}Th flux at 150 m estimated with ^{234}U concentrations and its decay constant in the upper water column (3.79 dpm m^{-2} yr^{-1}) [*Yu et al.*, 2001]. Although ^{230}Th method for trapping efficiency is usually applied to annual data [*Yu et al.*, 2001] and the above assumption is not always appropriate, it is likely that the trapping efficiency of the 150 m sediment trap was significantly low.

3.2. Relative Intensity of in situ QI

[5] Surface photosynthetically available radiation (PAR) obtained from SeaWiFS optical data generally increased from late March and reached maximum values in June (Figure 1). Surface PAR then tended to decrease. In situ QI at *ca.* 40 m was generally synchronized with surface PAR in April. However in situ QI decreased thereafter as opposed to increases of surface PAR and reached its minimum in late-June to early-July. In situ QI then increased again, peaking in mid-August. The relative decrease of in situ QI between late-April and early-August indicates increase of light attenuation or increase of turbidity in the water column above BLOOMS.

4. Discussion

4.1. Comparison of Optical Signals and Organic Carbon Fluxes

[6] It has been verified that Ed at *ca.* 440 nm is preferentially absorbed by pigments (chlorophyll) of principal phytoplankton as opposed to Ed at *ca.* 550 nm [*Kirk*, 1994]. Thus the ratio of Ed at 555 nm to that at 443 nm ($Ed_{(555)}/Ed_{(443)}$) serves as a good index of Chl-*a* [e.g., *Loisel and Morel*, 1998]. Using BLOOMS data, seasonal variability in the $Ed_{(555)}/Ed_{(443)}$ as proxies for Chl-*a* was evident (Figure 2). The $Ed_{(555)}/Ed_{(443)}$ began to increase in late-April and the maximum values were observed in late-June to early-July. This seasonal pattern correlated well with that of the surface PAR/in situ QI ratio (R = 0.94) and, moreover, that of the SeaWiFS-derived surface Chl-*a* in the vicinity of station K2 (R = 0.78, P < 0.001). This suggests that the increase of turbidity between the late-April and mid-August with maximum in July is likely attributable to increases of phytoplankton. As shown in Figure 2, seasonal variability in organic carbon flux (OCF) follows the same pattern as optical variability: OCF began to increase in late-April and increased more largely between the late-June and August. The correlation coefficient between OCF and the $Ed_{(555)}/Ed_{(443)}$ was found to be statistically significant (R = 0.62, P < 0.005). Based on good synchronization between seasonal patterns of OCF and optical signals, it is concluded that primary produced organic carbon in the euphotic layer was likely quickly transported to the ocean interior with time lag <1 week.

4.2. Estimation of Primary Productivity and Export Ratio

[7] Based on previous observations in the northern North Pacific (Figure 3), integrated Chl- *a* abundance (Chl-$a_{(int)}$) upper 40 m (mg m^{-2}) can be expressed as logarithmic function of the $Ed_{(555)}/Ed_{(443)}$ at 40 m:

$$\text{Chl-}a_{(\text{int})} = 29.89 + 33.375 \times \log\left(\text{Ed}_{(555)}/\text{Ed}_{(443)}\text{ratio}\right) \quad (1)$$

Using the following empirical equation, depth-integrated production in the upper 40 m (PP) can then be determined using equation 1 and daily surface PAR.

$$\text{PP} = \text{Chl-}a_{(\text{int})} \times \text{surface PAR} \times \Psi \quad (2)$$

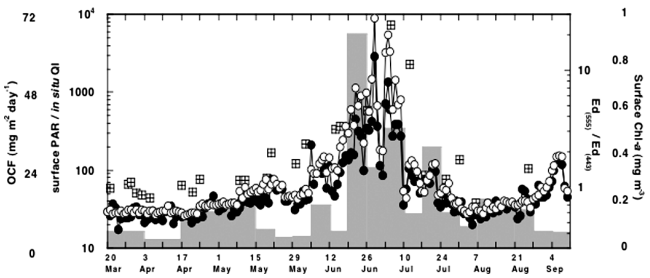

Figure 2. The $Ed_{(555)}/Ed_{(443)}$ (open circles), surface PAR/in situ QI ratios (closed circles), and Organic Carbon Flux (OCF) at 150 m (bar graphs). Squares are SeaWiFS derived surface Chl-*a*.

where Ψ is water column light utilization index [e.g., *Platt et al.*, 1988]. In this study, a constant value of Ψ (0.3 ± 0.1) reported by *Imai et al.* [2002] for the WSG was applied.

[8] Seasonal variability in estimated PP also shows similar pattern of the $Ed_{(555)}/Ed_{(443)}$ and Chl-$a_{(int)}$, resulting good synchronization of OCF (Figure 4). Minimum and maximum of PP were estimated to be *ca.* 50 mgC m^{-2} day^{-1} in late-March and *ca.* 1200 mgC m^{-2} day^{-1} in July, respectively. Mean PP was estimated to be 297 ± 99 mgC m^{-2} day^{-1}. This value was comparable to that observed in the WSG for the corresponding season (270 mgC m^{-2} day^{-1} [*Imai et al.*, 2002]). Figure 4 also shows PP estimated with satellite data and algorithm proposed by *Kameda and Ishizaka* [2005] ($PP_{(KI)}$) based on VGPM algorithm [*Behrenfeld and Falkowski*, 1997]. Though PP estimated in this study tends to be lower than $PP_{(KI)}$ after late-July and other factor such as temperature might be considered in equation 2, both estimates generally coincided well. Thus, the mean export ratio (ratio of mean OCF at 150 m, 13 mgC m^{-2} day^{-1}, to PP) was estimated to be 4 ± 1%. This export ratio was considerably smaller than the annual average of export ratio (*ca.* 45%) estimated using the seasonal amplitude of nutrients (new production) and the observed PP for the WSG [*Honda*, 2003]. However if trapping efficiency of our sediment trap was *ca.* 20% as described before, actual OCF at 150 m should be 5 times larger than the observed OCF, resulting in an export ratio of 22 ± 7%. Further, the export ratio of 45% by *Honda* [2003] was an estimate at 100 m. It has been reported that OCF decreases with depth [*Martin et al.*, 1987]. If decrease of OCF with depth can be formulated as a power function as proposed by them, OCF at 100 m becomes 1.4 times larger than OCF at 150 m. If this is the case, the OCF at 100 m is estimated to be *ca.* 90 mgC m^{-2} day^{-1} and becomes comparable to seasonal new production for the WSG (*ca.* 90 mgC m^{-2} day^{-1} [*Midorikawa et al.*, 2002]). Consequently, the export ratio is estimated to be *ca.* 31 ± 10%. This export ratio is significantly higher than that reported for other oceans (<10% [*Buesseler*, 1998]). Although many uncertainties remain, high export flux and ratio values in the WSG are supported by previous reports: export fluxes and ratios are high in the productive and diatom-dominant areas [*Buesseler*, 1998].

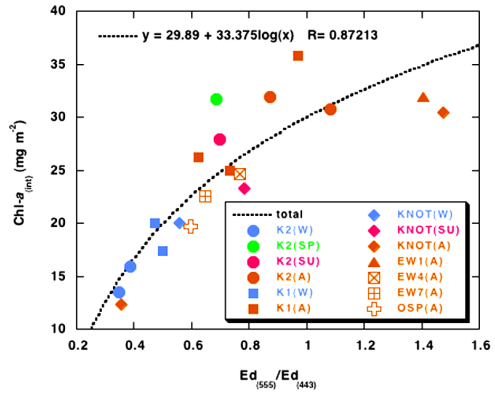

Figure 3. Relation between $Ed_{(555)}/Ed_{(443)}$ at 40 m and integrated Chl-*a* abundances upper 40 m (Chl-$a_{(int)}$). The $Ed_{(555)}/Ed_{(443)}$ were measured at 40 m with underwater optical sensor (Satlantic SeaWiFS Multichannel Radiometer), and Chl-*a* of discrete seawater samples upper 40 m were measured using Turner designs fluorometer aboard ship at various stations and seasons in the northern North Pacific during previous *R/V MIRAI* cruises [*Honda*, unpublished data]. Stations K2, K1, KNOT, EW1, EW4, EW7 and OSP are located at 47°N/160°E, 51°N/165°E, 44°N/155°E, 47°N/169°E, 46°N/175°W, 49–30°N/160°W and 50°N/145°W, respectively. W, SP, SU, and A in parenthesis indicate observation seasons of winter, spring, summer and autumn, respectively. Despite data collected at different locations and seasons, good correlation between $Ed_{(555)}/Ed_{(444)}$ and Chl-$a_{(int)}$ can be seen.

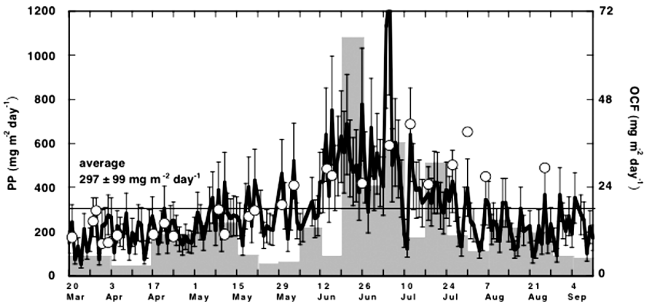

Figure 4. Seasonal variability in primary productivity estimated with the $Ed_{(555)}/Ed_{(443)}$ ratio and empirical equation (see text). Open circles are PP estimated with satellite data and algorithm [*Kameda and Ishizaka*, 2005]. Bar graphs are OCF at 150 m.

5. Concluding Remarks

[9] It was verified that measurement of optical fields in the water column was useful for the estimation of PP as a substitute for satellite data, and there is good evidence of quick transport of organic carbon assimilated in the euphotic layer to the ocean interior (at least to 150 m). For improved quantification, more data need to be accumulated; in particular, at least for one year's worth of data are needed especially for estimation of trapping efficiency. In addition, more precise values of Ψ are needed.

[10] **Acknowledgments.** We thank Susumu Honjo of Woods Hole Oceanographic Institution for promotion of our time-series observations. Derek Manov and Frank Spada of UCSB OPL provided technical support of the optical systems. We acknowledge Hiroaki Sakoh, Kazuhiro Hayashi, Toru Idai of Marine Works Japan and ship crews of *R/V MIRAI* for their efforts on maintenance of instruments, mooring system and mooring work. We appreciate anonymous reviewers for their constructive comments. Financial support for the development of the UCSB OPL optical instrumentation was provided in part by the U.S. National Science Foundation and the U.S. National Ocean Partnership Program.

References

Anderson, R. F., and A. P. Fleer (1982), Determination of natural actinides and plutonium in marine particulate material, *Anal. Chem.*, *54*, 1142–1147.

Banse, K., and D. C. English (1999), Comparing phytoplankton seasonality in the eastern and western Subarctic Pacific and the western Bering Sea, *Prog. Oceanogr.*, *43*, 235–288.

Behrenfeld, M. J., and P. G. Falkowski (1997), Photosynthetic rates derived from satellite-based chlorophyll concentration, *Limnol. Oceanogr.*, *42*(1), 1–20.

Buesseler, K. O. (1998), The decoupling of production and particulate export in the surface ocean, *Global Biogeochem. Cycles*, *12*(2), 297–310.

Dickey, T. D., et al. (2003), New sensors monitor bio-optical/biogeochemical ocean changes, *Sea Technol.*, *44*, 17–24.

Harrison, P. J., et al. (2004), Nutrient and plankton dynamics in the NE and NW gyres of the Subarctic Pacific ocean, *J. Oceanogr.*, *60*, 93–117.

Honda, M. C. (2003), Biological pump in northwestern North Pacific, *J. Oceanogr.*, *59*(5), 671–684.

Honda, M. C., et al. (2002), The biological pump in the northwestern North pacific based on fluxes and major component of particulate matter obtained by sediment trap experiments (1997–2000), *Deep Sea Res., Part II*, *49*, 5595–5625.

Honjo, S., et al. (1999), Monsoon-controlled export fluxes to the interior of the Arabian Sea: U.S. JGOFS 1994–1995 experiment, *Deep Sea Res., Part II*, *46*(8–9), 1859–1902.

Imai, K., et al. (2002), Time series of seasonal variation of primary productivity at station KNOT (44°N, 155°E) in the sub-arctic western North Pacific, *Deep Sea Res., Part II*, *49*, 5395–5408.

Kameda, T., and J. Ishizaka (2005), Size-fractionated primary production estimated by a two-phytoplankton community model applicable to ocean color remote sensing, *J. Oceanogr.*, *61*, 663–672.

Kirk, J. T. O. (1994), *Light and Photosynthesis in Aquatic Ecosystem*, 2nd ed., pp. 305–313, Cambridge Univ. Press, New York.

Loisel, H., and A. Morel (1998), Light scattering and chlorophyll concentration in case 1 water: A reexamination, *Limnol. Oceanogr.*, *43*, 847–858.

Manov, D., et al. (2004), Methods for reducing biofouling on moored optical sensors, *J. Atmos. Oceanic Technol.*, 957–967.

Martin, J. H., et al. (1987), VERTEX: Carbon cycling in the northeast Pacific, *Deep Sea Res., Part A*, *34*, 267–285.

Midorikawa, T., et al. (2002), Estimation of seasonal net community production and air-sea CO_2 flux based on the carbon budget above the temperature minimum layer in the western subarctic North Pacific, *Deep Sea Res., Part I*, *49*, 339–362.

Platt, T., et al. (1988), Ocean primary productivity and available light: Further algorisms for remote sensing, *Deep Sea Res., Part II*, *35*, 855–879.

Sorensen, J. C., and D. A. Siegel (2001), Variability of the effective quantum yield for carbon assimilation in the Sargasso Sea, *Deep-Sea Res., Part II*, *48*, 2005–2035.

Volk, T., and M. I. Hoffert (1985), Ocean carbon pumps: Analysis of relative strengths and efficiencies in ocean-driven atmospheric CO_2 changes, in *The Carbon Cycle and Atmospheric CO_2: Natural Variations Archean to Present*, *Geophys. Monogr. Ser.*, vol. 32, edited by E. Sundquist and W. S. Broecker, pp. 99–110, AGU, Washington, D. C.

Yu, E. F., et al. (2001), Trapping efficiency of bottom tethered sediment traps estimated from the intercepted fluxes of ^{230}Th and ^{231}Pa, *Deep Sea Res., Part I*, *48*, 865–889.

T. Dickey, Ocean Physics Laboratory, University of California, Santa Barbara, 6487 Calle Real, Unit A, Goleta, CA 93117, USA.

M. C. Honda, H. Kawakami, and S. Watanabe, Mutsu Institute for Oceanography, Japan Agency for Marine-Earth Science and Technology, 2-15, Natsushima, Yokosuka, Kanagawa 237-0061, Japan. (hondam@jamstec.go.jp)

K. Sasaoka, Frontier Research Center for Global Change, Japan Agency for Marine-Earth Science and Technology, 3173-25, Showa, Kanazawa, Yokohama 236-0001, Japan.